Atherosclerosis 285 (2019) 108–119

Contents lists available at ScienceDirect

Atherosclerosis

journal homepage: www.elsevier.com/locate/atherosclerosis

FcγRIIb on CD11c$^+$ cells modulates serum cholesterol and triglyceride levels and differentially affects atherosclerosis in male and female *Ldlr*$^{-/-}$ mice

Jennifer Marvin[b], Jillian P. Rhoads[b], Amy S. Major[a,b,*]

[a] Tennessee Valley Healthcare System, U.S. Department of Veterans Affairs, Nashville, TN, 37212, USA
[b] Department of Medicine, Division of Rheumatology and Immunology, Vanderbilt Medical Center, Nashville, TN, 37232, USA

HIGHLIGHTS

- Female *CD11c-Cre*$^+$ *Fcgr2b*$^{fl/fl}$ recipients have larger plaques than control mice.
- Male *CD11c-Cre*$^+$ *Fcgr2b*$^{fl/fl}$ recipients have smaller plaques than control mice.
- CD11c-specific FcγRIIb alters hepatic inflammation differently in males and females.
- A CD11c-conditional FcγRIIb knockout decreases serum lipoproteins in both sexes.
- Liver lipid synthesis and handling are altered in *CD11c-Cre*$^+$ *Fcgr2b*$^{fl/fl}$ recipients.

ARTICLE INFO

Keywords:
Atherosclerosis
Dendritic cells
FcγRIIb
Hepatic cholesterol

ABSTRACT

Background and aims: Circulating levels of oxidized lipoprotein (oxLDL) correlate with myocardial infarction risk and atherosclerosis severity. Our previous study demonstrates that oxLDL immune complexes (oxLDL-ICs) can signal through FcγRs on bone marrow-derived dendritic cells (BMDCs) and enhance their activation and inflammatory cytokine secretion. While global *FcγR*$^{-/-}$ studies have shown that activating FcγRs are proatherogenic, the role of the inhibitory FcγRIIb is unclear. We sought to determine the role of DC-specific FcγRIIb in atherosclerosis.

Methods: Bone marrow chimeras were generated by rescuing lethally irradiated *Ldlr*$^{-/-}$ mice with hematopoietic cells from littermate *CD11c-Cre*$^+$ or *CD11c-Cre*$^-$ *Fcgr2b*$^{fl/fl}$ donors. Four weeks following transplant, recipients were placed on a Western diet for eight weeks. Various tissues and organs were analyzed for differences in inflammation.

Results: Quantitation of atherosclerosis in the proximal aorta demonstrated a 58% increase in female *CD11c-Cre*$^+$ *Fcgr2b*$^{fl/fl}$ recipients, but a surprising 44% decrease in male recipients. Hepatic cholesterol and triglycerides were increased in female *CD11c-Cre*$^+$ *Fcgr2b*$^{fl/fl}$ recipients. This was associated with an increase in CD36 and MHC Class II expression on hepatic CD11c$^+$CD11b$^+$ DCs in female livers. In contrast, male *CD11c-Cre*$^+$ *Fcgr2b*$^{fl/fl}$ recipients had decreased hepatic lipids with a corresponding decrease in CD36 and MHC Class II expression on CD11c$^+$ cells. Interestingly, both sexes of *CD11c-Cre*$^+$ *Fcgr2b*$^{fl/fl}$ recipients had significant decreases in serum cholesterol and TGs with corresponding decreases in liver *Fasn* transcripts.

Conclusions: The absence of FcγRIIb expression on CD11c$^+$ cells results in sex-dependent alteration in liver inflammation influencing atherogenesis and sex-independent modulation of serum cholesterol and TGs.

1. Introduction

Cardiovascular disease (CVD) leads all-cause mortality in both men and women in the U.S, claiming more lives than cancer and chronic respiratory lung disease combined. The American Heart Association predicts that by 2035, over 130 million American adults (45.1%) will have some form of CVD [1]. Atherosclerosis is a chronic inflammatory disease of the vessel wall that underlies the vast majority of CVD disorders. Cholesterol, and in particular, oxidized lipoproteins (oxLDL) are well established mediators of atherosclerotic plaque formation. Interestingly, up to 90% of circulating oxLDL can complex with specific antibodies to form oxLDL immune complexes (oxLDL-ICs) [2]. These ICs have long been known to positively correlate with myocardial infarction risk, carotid atherosclerosis severity, and poor CVD outcomes

* Corresponding author. Vanderbilt University, 1161 21st Avenue South, A-3314 Medical Center North, Nashville, TN, 37232, USA.
E-mail address: amy.major@vumc.org (A.S. Major).

https://doi.org/10.1016/j.atherosclerosis.2019.04.221
Received 19 December 2018; Received in revised form 8 April 2019; Accepted 12 April 2019
Available online 13 April 2019

[2,3]. Despite this, oxLDL-ICs have only recently been implicated in disease pathogenesis. OxLDL-ICs were found to be more potent primers of the NLRP3 inflammasome and elicited greater IL-1β production than free oxLDL in bone marrow-derived dendritic cells (DCs) [4]. However, the mechanism behind oxLDL-ICs enhanced inflammatory effects is unknown.

Our data suggest that oxLDL-ICs' effects are partially mediated via Fc gamma receptors (FcγRs). FcγRs are found on antigen presenting cells (APCs) such as macrophages, DCs, and B-cells and have high affinity for the Fc region of IgG antibodies. *In vitro* studies demonstrate that oxLDL-ICs can signal through Fc receptors in both human macrophage cells lines and murine bone marrow-derived DCs, likely in concert with toll-like receptor 4 and the scavenger receptor CD36 [4,5]. FcγRs can be either activating or inhibitory, containing an immunoreceptor tyrosine-based activation motif or an immunoreceptor tyrosine inhibitory motif, respectively [6]. The activating murine FcγRs, FcγRI, FcγRIII, and FcγRIV, have been shown to be proatherogenic [7].

The lone inhibitory FcγR, FcγRIIb, is well conserved across species, and is present on most immune cells [6]. It is the only FcγR expressed on B-cells and has been studied most extensively in relation to autoimmune diseases. Global *FcγRIIb*$^{-/-}$ mice develop a spontaneous lupus-like phenotype with elevated anti-nuclear antibody titers and glomerulonephritis [8]. Additionally, polymorphisms in *Fcgr2b* are associated with susceptibility to systemic lupus erythematosus (SLE) and rheumatoid arthritis in humans [9–11]. Although the inhibitory FcγRIIb is expressed at lower levels compared to the activating FcγRs in bone marrow-derived DCs, several studies support a role for FcγRIIb in regulating DC function [4]. In a bovine type II collagen-induced model, CD11c-conditional FcγRIIb knockout (KO) mice were more susceptible to developing arthritis [12]. Furthermore, FcγRIIb knockout mice demonstrated increased dermal DC migration to lymph nodes [13]. DC FcγRIIb is also reported to strongly regulate the other activating FcγRs *in vitro* [14]. These data highlight a role for FcγRIIb in regulating DCs.

The impact of FcγRIIb on atherogenesis, however, remains unclear. Male *Apoe*$^{-/-}$*Fcgr2b*$^{-/-}$ mice placed on a Western diet experience increased atherosclerosis independent of lipid levels, characterized by increased antibody titers and pro-inflammatory cytokines in the aorta [15]. Conversely, a separate group reported that *Apoe*$^{-/-}$*Fcgr2b*$^{-/-}$ mice demonstrated decreased carotid and aortic root atherosclerosis, with higher numbers of circulating T_{REGS} and higher serum levels of IL-10 and TGF-β [16,17]. The authors suggested that these conflicting results are likely due to strain differences, as the former may have increased expression of lupus-associated *Slam* genes located near *Fcgr2b* while the latter did not [17].

Given that oxLDL-IC stimulation of FcγRs on DCs affected inflammasome activation, cytokine production, and downstream T-cell responses *in vitro*, we sought to determine how FcγRIIb expression on DCs impacts atherosclerosis *in vivo*. We hypothesized that a conditional knockout of this inhibitory receptor in DCs would result in increased atherosclerosis. Surprisingly, we found that female *Ldlr*$^{-/-}$ recipients of *CD11c-Cre*$^{+}$ *Fcgr2b*$^{fl/fl}$ bone marrow experienced increased atherosclerosis, while male *Ldlr*$^{-/-}$ recipients of *CD11c-Cre*$^{+}$ *Fcgr2b*$^{fl/fl}$ bone marrow had an unexpected decrease in atherosclerosis compared to littermate controls. Changes in atherosclerosis occurred despite both sexes having improved serum cholesterol and triglyceride profiles with CD11c^{+} specific FcγRIIb knockdown. Instead, atherosclerosis seemed to be more related to sex-specific differences in APC functional markers within the liver. Collectively, these findings support a novel role for FcγRIIb in CD11c^{+} cells for maintaining liver cholesterol homeostasis and reveal unexpected sex-dependent differences in the inflammatory response during atherosclerosis.

2. Materials and methods

2.1. Mice

C57BL/6J-Tg Itgax-cre,-EGFP 4097Ach/J (*CD11c-Cre-GFP*; Stock # 007567*)* and B6.129S7-*Ldlr*^{tm1Her}/J (*Ldlr*$^{-/-}$; Stock # 002207*)* mice were originally obtained from the Jackson Laboratory (Bar Harbor, ME). Mice homozygous for the *Fcgr2b*^{fl} alleles were generously gifted from Jeffery V. Ravetch (The Rockefeller University, New York City, NY) and bred with *CD11c-Cre*$^{+}$ mice to obtain *CD11c-Cre*$^{+}$ *Fcgr2b*$^{fl/fl}$ mice and *CD11c-Cre*$^{-}$ mice as determined by PCR. (Please see Major Resources Table in the Supplemental Material). All mice were subsequently housed and maintained at Vanderbilt University. Procedures were approved by the Vanderbilt University Institutional Animal Care and Use Committee.

2.2. Bone marrow transplants and atherosclerosis quantification

Eight to twelve-week-old *Ldlr*$^{-/-}$ mice were lethally irradiated (900 rad) by a ^{137}Cs source. After 4 h, up to 5 × 10^{6} bone marrow cells harvested from the femurs of *CD11c-Cre*$^{+}$ *Fcgr2b*$^{fl/fl}$ mice or *CD11c-Cre*$^{-}$ littermates were transferred into irradiated *Ldlr*$^{-/-}$ recipients via retro-orbital injection. Transplanted mice were cohoused and maintained on a normal chow diet for 4–5 weeks during reconstitution. Following reconstitution, mice were placed on a Western diet (21% saturated fat, 0.15% cholesterol, TD.88,137, Envigo, Indianapolis, IN). Mice were sacrificed after 8 weeks of Western diet and atherosclerotic lesion burden was quantified in the proximal aorta by oil-red-O staining as previously described [18].

2.3. Serum amyloid A and anti-oxLDL antibody ELISAs

Serum Amyloid A was measured using a commercially available kit (Abcam, Cambridge, MA) and following the manufacturer's instructions. Samples were assessed at a 1:1000 dilution.

For anti-oxLDL antibody ELISAs, Nunc MaxiSorp plates were coated with 10 μM oxLDL at 4 °C overnight. OxLDL was generated as previously described [4]. Plates were washed three times in PBS containing 0.05% Tween and blocked in 1% BSA/PBS (Fisher Scientific, Waltham, MA) at room temperature (RT) for 2 h. Plates were washed in PBS-Tween x3 and serum samples diluted in 1% BSA/PBS were added and incubated for 2 h at RT. Plates were washed five times with PBS-Tween. For Total IgG quantification, anti-mouse IgG-HRP (Promega, Madison, WI) diluted 1:5000 was added to the wells and incubated overnight at 4 °C. Plates were washed with PBS-Tween x5 and OptEIA TMB substrate (BD Biosciences, San Diego, CA) was added. Plates developed for 10 min prior to quenching with 2M HCl and immediately read at 450 nM.

For IgM and IgA quantification, goat anti-mouse IgA-biotin (Southern Biotechnology, Birmingham, AL) and goat anti-mouse IgM biotin (Southern Biotechnology) were added at a 1:5000 dilution to the wells overnight at 4 °C. Plates were washed with PBS-Tween x5 and incubated with streptavidin-peroxidase (MilliporeSigma, St Louis, MO) at 2.5 μg/mL for 30 min at RT. Plates were developed for 25 min in TMB substrate and quenched as described above.

2.4. Macrophage immunohistochemistry

5 μM sections of the proximal aorta were fixed in cold acetone and incubated at room temperature in 2% BSA/PBS. Slides were treated with avidin block (Vector, Olean, NY), biotin block (Vector), and peroxidase-activity block (9:1 ratio of methanol:30% H_2O_2). Macrophages were stained using a 1:25 dilution of rat-anti mouse macrophage/monocyte, clone MOMA-2 (MilliporeSigma) in 2% BSA/PBS for 1 h at RT. Next, slides were stained with a 1:200 dilution of biotin goat-anti rat (BD Biosciences) in 2% BSA/PBS for 30 min at 37 °C. Strepavadin-

HRP (Biogenex, Fremont, CA) was applied for 20 min followed by AEC substrate (Abcam) for 2 min. Hematoxylin counterstain was applied for 2 min and slides were imaged using a Q-Color5™ imaging system (Olympus, Center Valley, PA). Quantification of macrophage/monocyte area was performed using ImageJ and averaged for four sections.

2.5. Serum, liver, and fecal cholesterol and triglyceride assays

Mice were fasted on paper bedding for 4 h and blood was collected via the retroorbital sinus. Lipids were extracted from stool samples and liver segments using a modified version of Folch-Lees [19]. Briefly, 10 mg aliquots of feces dried at 70 °C for 1 h were crushed into a powder, resuspended in 2:1 chloroform-methanol, and incubated at 60 °C for 30 min under constant agitation. The suspension was centrifuged at 1000 × *g* for 10 min and water was added to the supernatant. Phase separation was induced by low-speed centrifugation and the chloroform phase was removed and evaporated until dry. Samples were re-suspended in chloroform-2% Triton X-100, evaporated until dry, and then resuspended in diH_2O with 2% Triton X-100. For the liver segments, 50–100 mg aliquots of tissue were homogenized in 2:1 chloroform-methanol and agitated overnight on an orbital shaker at 4 °C and then treated as described above. Cholesterol and triglycerides were measured using a commercially available kit (Raichem, San Marcos, CA).

2.6. Isolation of serum lipoproteins by FPLC

Size-exclusion chromatology was carried out on a Superose 6 10/300 GL column (GE Healthcare, Uppsala, Sweden) and elutions monitored at an absorbance of 280 nm. Samples were prepared for injection by thawing on ice, centrifuging at 10,000 × *g* for 5 min, and pooling two samples to reach a total volume of 100 μL. Collected fractions were analyzed for cholesterol and triglyceride content using the commercially available kits as described above.

2.7. Isolation of immune cells from livers and adipose tissue

Livers were perfused through the heart with PBS, minced, and digested in 1 mg/mL of Collagenase, type II (Worthington Biochemical, Lakewood, NJ) in HBSS with calcium and magnesium for 30 min at 37 °C. Liver tissue was passed through a 40 μM strainer and debris was separated by decanting. Cells were collected by centrifugation at 1500 rpm for 10 min and subsequently resuspended in 40% Percoll. After underlaying a layer of 60% Percoll, the gradient was spun at 2000 rpm for 20 min. Leukocytes were collected from the interface of the 40% and 60% layers.

Gonadal fat pads were harvested and processed as previously described [20]. Briefly, fat pads were minced in 1% FBS in PBS and then digested in 2 mg/mL of Collagenase, type II (Worthington Biochemical) for 40 min at 37 °C in a rotational shaker at 200 rpm. The homogenate was triturated several times before passing through a 40 μM strainer. RBCs and adipocytes were lysed by resuspension in ACK buffer (Gibco, Langley, OK) for 3 min on ice. Cells were then passed through a FACS filter cap prior to staining.

2.8. Flow cytometry

Flow cytometry was performed on leukocytes isolated from organs as described above. Cells were washed in FACS buffer containing HBSS, 1% BSA, 4.17 mM sodium bicarbonate, and 3.08 mM sodium azide and incubated for 15 min at room temperature with Fc Block (anti-CD16/32; Tonbo, San Diego, CA) except for stains for FcγRIIb. Cells were then incubated for 30 min at 4 °C with the following antibodies: anti-CD11c-FITC (Tonbo), anti-CD11b-V450 (Tonbo), anti-CD45.2-APCCy7 (Tonbo), anti-CD64-PE (BD, San Jose, CA), anti-CD36-APC (BD), anti-MHC Class II-PerCP-Cyanine5.5 (Tonbo), anti-CD32b-PE (Thermofisher, Waltham, MA), anti-TCRβ-V450 (Tonbo), and anti-CD4-PeCy7 (Tonbo). All samples were washed, and either fixed in 2% paraformaldehyde (PFA) or permeabilized using the Foxp3/Transcription Factor Staining Buffer Set (eBioscience, San Diego, CA) for intracellular staining overnight at 4 °C. Cells were then stained an additional 30 min with anti-FoxP3-FITC (eBioscience) followed by washing and fixation in 2% PFA. Samples were run using a MACSQuant Analyzer (Miltenyi, Auburn, CA) and analyzed using FlowJo software.

2.9. Liver qPCR

10 mg liver segments were stored at −20 °C in RNA*later* Solution (Thermofisher) until RNA was purified using the tissue protocol from the Norgen Biotek Total RNA Purification Kit (Ontario, Canada). RNA concentrations were normalized, and RNA was reversed transcribed with a High-Capacity RNA-to-cDNA kit (Applied Biosystems, Grand Island, NY). The reverse transcription product was used for detecting mRNA expression by quantitative real-time PCR with TaqMan™ probes (Thermofisher) for *Fasn, Msr1, Abca1, Abcg1, Cd36, Hmgcr, and Srebp1* on the QuantStudio 6 Flex Real-Time PCR System (Life Technologies). The cycling-threshold (C_T) value for each gene was normalized to the housekeeping gene *Ppia*, and the relative expression was calculated by the change in cycling threshold method (ΔΔCT). Probe catalog numbers can be found in the supplemental methods.

2.10. Statistical analyses

Statistical significance between experimental and control groups was determined using a Student's *t*-test normally distributed data and A Mann-Whitney test for non-normally distributed data in Graph Pad Prism (San Diego, CA).

3. Results

3.1. FcγRIIb expression on CD11c$^+$ cells modulates atherosclerosis in a sex-dependent manner

To study the effects of FcγRIIb expression in CD11c$^+$ cells on atherosclerosis, we generated bone marrow chimeras with *Ldlr*$^{-/-}$ recipients and *CD11c-Cre*$^+$ *Fcgr2b*$^{fl/fl}$ or littermate control CD11c-*Cre*$^-$ donors (Fig. 1A). Transplanted mice were cohoused and fed a Western diet for 8 weeks. Flow cytometry on splenic and hepatic leukocytes confirmed reduced FcγRIIb expression on CD11c^{hi} CD11b^{hi} expressing cells in both female and male recipients (Fig. 1B–C). Quantification of atherosclerosis by Oil-red-O (ORO) area and total lesion area in the aortic root resulted in a near 60% increase in total atherosclerotic lesion size in female recipients of *CD11c-Cre*$^+$ *Fcgr2b*$^{fl/fl}$ bone marrow (Fig. 1D–E). However, male recipients of *CD11c-Cre*$^+$ *Fcgr2b*$^{fl/fl}$ bone marrow had an unexpected 44% decrease in total lesion area.

3.2. CD11c-Cre$^+$ Fcgr2b$^{fl/fl}$ recipients have sex-dependent differences in serum markers of inflammation and macrophage composition in the proximal aorta

To determine if the differences in atherosclerosis could be attributed to differences in inflammation, we measured serum cytokine and amyloid A levels. While no differences were observed in serum IFNγ, IL-1β, IL-6, IL-10, IL-17A, IL-23, or TNFα between *CD11c-Cre*$^+$ *Fcgr2b*$^{fl/fl}$ recipients and controls (Supplemental Fig. 1A), female *CD11c-Cre*$^+$ *Fcgr2b*$^{fl/fl}$ recipients had significantly elevated serum amyloid A levels (Fig. 2A). There were no differences in serum amyloid A levels in male recipients.

Given our previous work with oxLDL-ICs *in vitro* [4], we hypothesized that there may be differences in anti-oxLDL antibody titers. Serum studies revealed elevated anti-oxLDL IgM in male *CD11c-Cre*$^+$ *Fcgr2b*$^{fl/fl}$ recipients with a trend towards decreased anti-oxLDL IgM in female

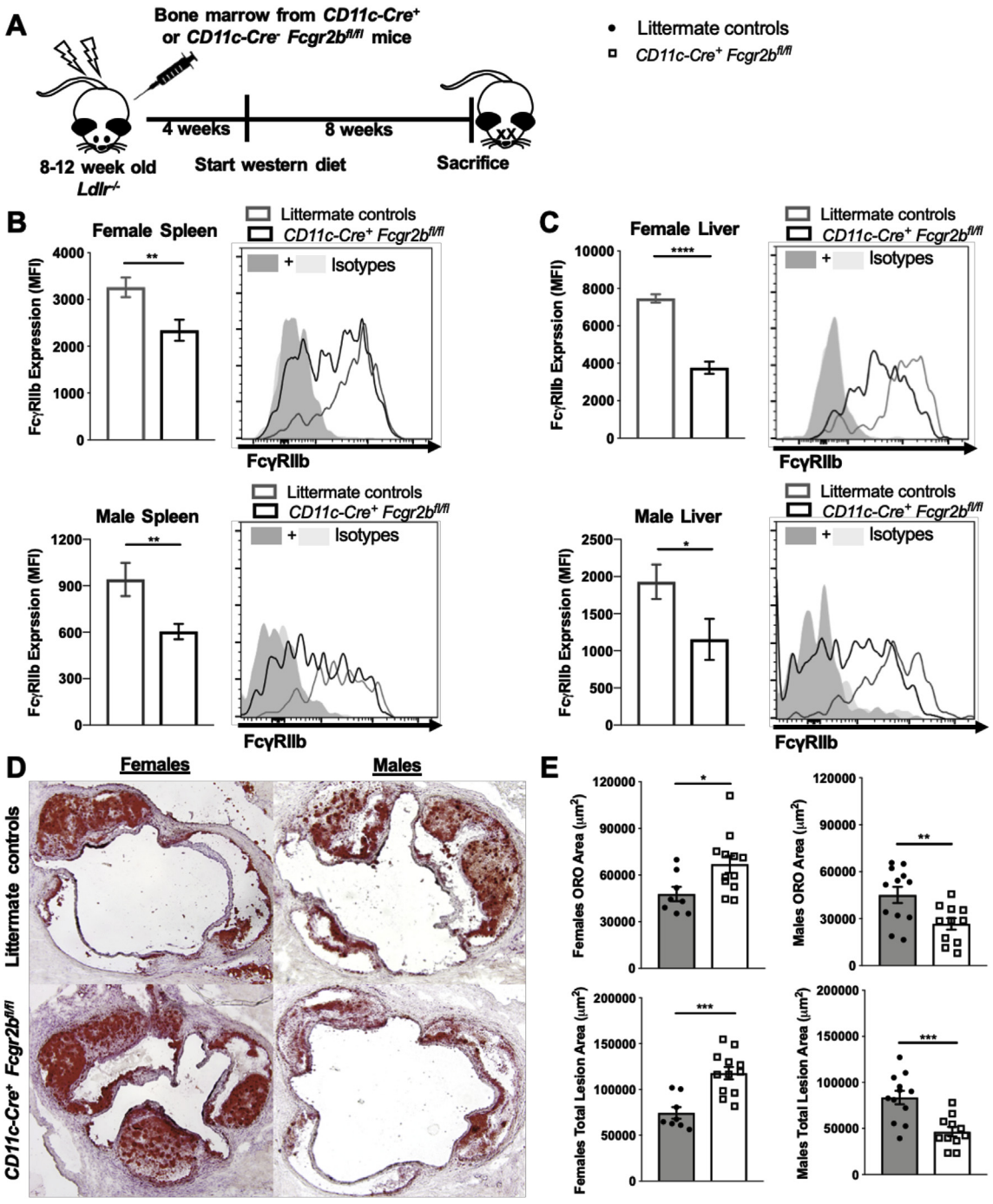

Fig. 1. Sex influences the impact of a CD11c conditional FcγRIIb KO on atherosclerosis.
(A) Study design. Bone marrow from 5-week old *CD11c-Cre*$^{+}$ and *CD11c-Cre*$^{-}$ *Fcgr2b*$^{fl/fl}$ mice was transplanted into lethally irradiated 8-12-week-old male and female *Ldlr*$^{-/-}$ mice. After 4–5 weeks of reconstitution on a normal chow diet, mice were fed a Western diet for 8 weeks prior to euthanasia. (n = 8–12 mice per group, 3 independent experiments) (B) Spleen FcγRIIb expression in CD11c^{hi} CD11b^{hi} cells from *CD11c-Cre*$^{+}$ *Fcgr2b*$^{fl/fl}$ and littermate control bone marrow recipients quantified by mean fluorescence intensity (MFI). (C) Liver FcγRIIb expression on CD11c^{hi} CD11b^{hi} cells from *CD11c-Cre*$^{+}$ *Fcgr2b*$^{fl/fl}$ recipients quantified by MFI. (D) Representative Oil-Red-O stained atherosclerotic lesions from the aortic root, quantified in (E) by Oil-Red-O (ORO) area and total lesion area. Error bars shown above represented standard error. *, **, and *** indicate significance at $p < 0.05$, $p < 0.01$, and $p < 0.001$ respectively by Student's *t*-test.

recipients (Fig. 2B). There was no difference in anti-oxLDL IgG, IgA or any of the IgG subtypes (Fig. 2B, Supplemental Fig. 1B). No differences were seen in immune cell composition or DC activation markers in the spleens of *CD11c-Cre*$^{+}$ *Fcgr2b*$^{fl/fl}$ recipients compared to controls (Supplemental Fig. 2).

Immunohistochemistry of the proximal aortic plaques showed that macrophages composed less of the total lesion in female *CD11c-Cre*$^{+}$ *Fcgr2b*$^{fl/fl}$ recipients (Fig. 2C). However, as the female lesions were greater in size, the total macrophage area was the same. Conversely, macrophages made up the same percentage of the plaque area in males, but because there was less atherosclerosis in the male *CD11c-Cre*$^{+}$ recipients, there was a decreased total macrophage area in male mice (Fig. 2C).

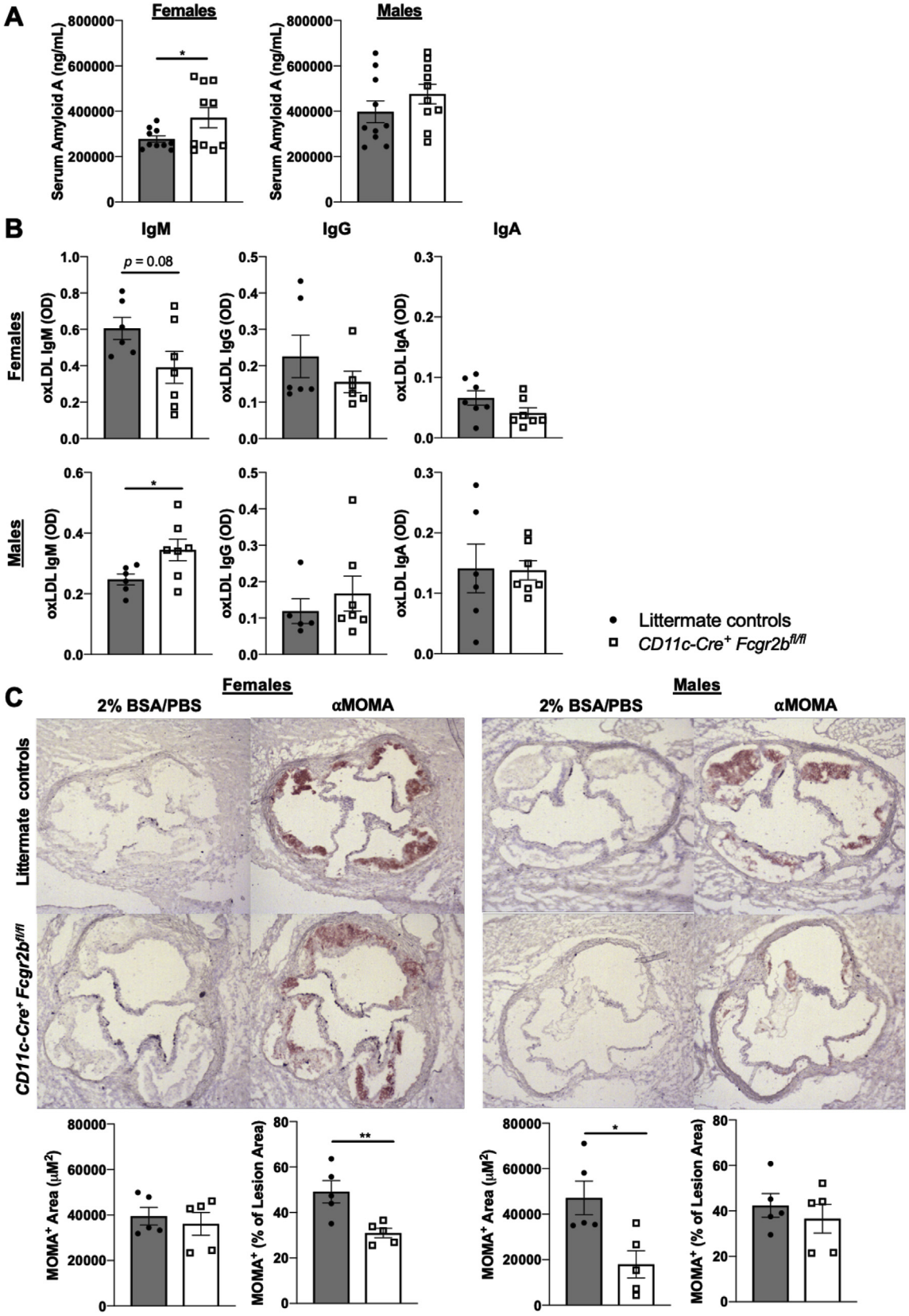

Fig. 2. Sex differences in serum markers of inflammation and macrophage infiltrate in atherosclerotic lesions.
(A) Serum amyloid A was measured using a commercially available kit. (B) Serum anti-oxLDL IgM, IgG, and IgA was determined by ELISA at a 1:50, 1:250, and 1:50 dilution respectively. (C) Macrophages in the proximal aorta were quantified by immunohistochemistry. 5 μM sections were stained with 2% BSA/PBS (left panels) or anti-mouse Macrophage/Monocyte (MOMA) (right panels). Slides were developed using AEC substrate and counterstained with hematoxylin. Quantification was performed based on total red area and % of lesion area. Error bars shown above represented standard error. * and ** indicate significance at $p < 0.05$ and $p < 0.01$ respectively, by Student's *t*-test.

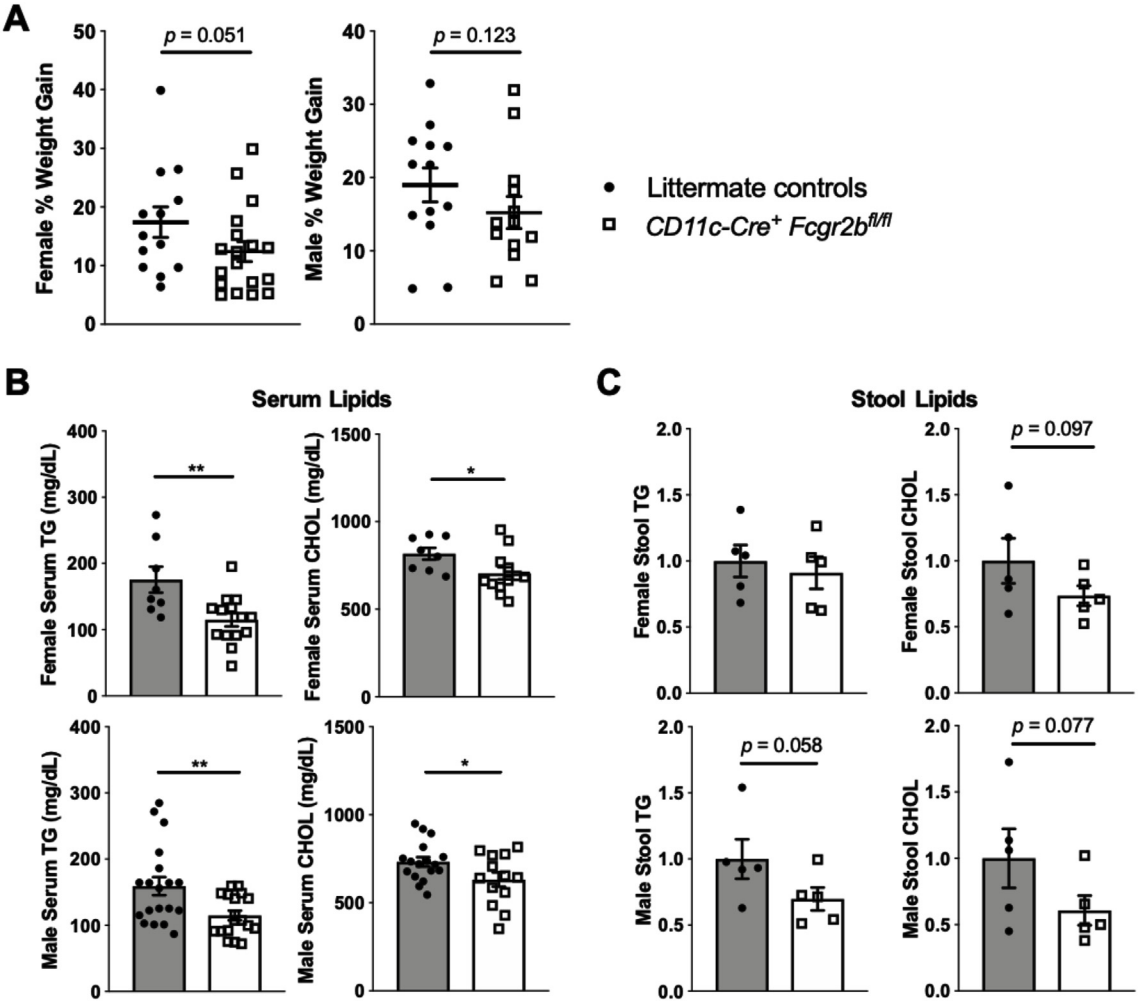

Fig. 3. *CD11c-Cre*$^{+}$ *Fcgr2b*$^{fl/fl}$ recipients gain less weight, have improved serum lipid profiles, and excrete less cholesterol.
(A) Percent weight gain of female and male mice after 8 weeks of Western diet. (B) Serum triglyceride (TG) and cholesterol (CHOL) after 8 weeks of Western diet for female mice (upper panels) and male mice (lower panels) as measured by commercially available kits. (C) Triglycerides (TG) and cholesterol (CHOL) excreted in the stool of *CD11c-Cre*$^{+}$ *Fcgr2b*$^{fl/fl}$ recipients and littermate controls after 8 weeks of Western diet. Lipids were extracted from 10 mg aliquots of dried stool collected after fasting using a modified version of the Folch method in 2:1 chloroform-methanol. Values are normalized to littermate controls. Error bars shown above represented standard error. * and **indicate significance at $p < 0.05$ and $p < 0.01$ by Student's *t*-test.

3.3. CD11c-Cre^{+} *Fcgr2b*$^{fl/fl}$ *recipients gain less weight, have improved serum lipid profiles, and excrete less cholesterol irrespective of sex*

Although we observed sex differences in atherosclerosis, both sexes trended towards less weight gain with a CD11c-conditional FcγRIIb KO (Fig. 3A). Despite this, *CD11c-Cre*$^{+}$ *Fcgr2b*$^{fl/fl}$ recipients did not have any differences in gonadal fat pad weight (Supplemental Fig. 3A). Male *CD11c-Cre*$^{+}$ *Fcgr2b*$^{fl/fl}$ recipients did have smaller spleen and liver masses compared to littermate controls, however, no differences were seen between female cohorts (Supplemental Figs. 3B–C).

We also examined the serum lipid profiles of the transplanted mice. In both sexes, *CD11c-Cre*$^{+}$ *Fcgr2b*$^{fl/fl}$ recipients had a substantial decrease in fasting serum triglycerides and a slight, but significant, decrease in serum cholesterol (Fig. 3B). FPLC analysis demonstrated that this reduction was present in both VLDL-TG and LDL-CHOL fractions, but not in HDL (Supplemental Figs. 4C–D). This improved serum lipid profile was surprising given that female *CD11c-Cre*$^{+}$ *Fcgr2b*$^{fl/fl}$ recipients had increased atherosclerosis. Because decreased circulating lipid may result from increased excretion in feces, stool samples were collected and analyzed for cholesterol content. Even prior to starting a Western diet, *CD11c-Cre*$^{+}$ *Fcgr2b*$^{fl/fl}$ recipients excreted less cholesterol, despite having similar serum cholesterol levels at baseline (Supplemental Figs. 4A–B). After 8 weeks of Western diet, both male and female *CD11c-Cre*$^{+}$ *Fcgr2b*$^{fl/fl}$ recipients continued to trend towards decreased stool lipid excretion (Fig. 3C). These results indicate that improved serum lipids in *CD11c-Cre*$^{+}$ *Fcgr2b*$^{fl/fl}$ recipients is not due to increased excretion through feces, but is rather likely related to lipid production, handling, or storage.

3.4. CD11c-Cre^{+} *Fcgr2b*$^{fl/fl}$ *recipients have increased pro-inflammatory dendritic cells in their adipose tissue*

Given the effect of a CD11c-conditional FcγRIIb KO on weight gain and serum lipids, APC populations were analyzed in white adipose tissue (WAT), as WAT is an important site of triglyceride and free fatty acid storage [21]. Studies were focused on the gonadal fat pads as those are often the first to develop signs of inflammation and insulin resistance among fat tissues [22]. There was a substantial increase in the percent of CD11c^{hi} CD11b^{hi} expressing cells in *CD11c-Cre*$^{+}$ *Fcgr2b*$^{fl/fl}$ recipients regardless of sex (Fig. 4A and Supplemental Fig. 5). As both AT macrophages (ATMs) and AT dendritic cells (ATDCs) can express CD11c and CD11b, we used CD64 to distinguish between ATMs (CD11c^{hi} CD11b^{hi} CD64^{+} cells) and ATDCs (CD11c^{hi} CD11b^{hi} CD64^{-} cells) [23]. We observed a significant decrease in the percent of ATMs

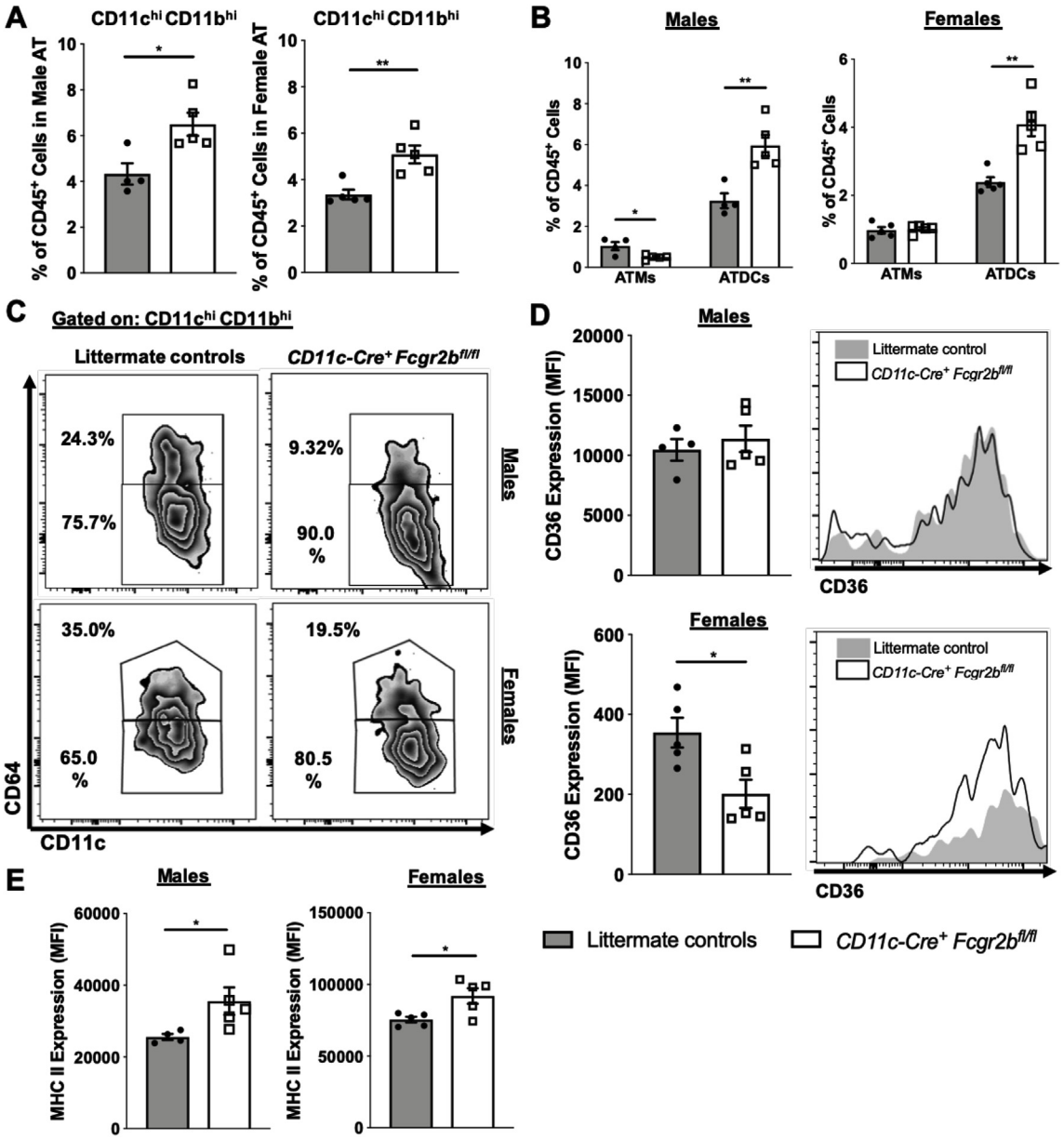

Fig. 4. *CD11c-Cre$^+$ Fcgr2b$^{fl/fl}$* recipients have increased pro-inflammatory dendritic cells in their white adipose tissue (WAT).
Gonadal fat pads from transplanted mice were digested with collagenase, 40 μM cell strainer passage, and RBC/adipocyte lysis prior to staining with CD45.2, CD11c, CD11b, CD64, MHC Class II, and CD36 by flow cytometry. (A) Percent of CD45$^+$ cells that are CD11c^{hi} CD11b^{hi} in male WAT (left) and female WAT (right). (B) Percent of CD11c^{hi} CD11b^{hi} CD64$^+$ macrophages and CD11c^{hi} CD11b^{hi} CD64$^+$ dendritic cells of CD45$^+$ cells in male and female WAT. (C) Representative contour plots of CD11c versus CD64 (gated on CD11c^{hi} CD11b^{hi}) to examine ATM and ATDC populations. (D) CD36 expression on CD11c^{hi} CD11b^{hi} CD64$^+$ WAT macrophages in male mice (upper panels) and female mice (lower panels) quantified by MFI. (E) MHC Class II expression on CD11c^{hi} CD11b^{hi} CD64$^-$ WAT dendritic cells in male (left) and female mice (right) quantified by MFI. Data are representative of N = 4–5 mice per group. Error bars shown above represent standard error. * indicates $p < 0.05$ and ** $p < 0.01$ by Student's *t*-test.

with a concurrent increase in ATDCs in male WAT (Fig. 4B–C). WAT from female *CD11c-Cre$^+$ Fcgr2b$^{fl/fl}$* recipients also demonstrated a two-fold increase in percent of ATDCs but showed no change ATMs. ATDCs are known to accumulate in WAT in obesity and are the dominant CD11c$^+$ population with moderate high fat diet exposure, which is consistent with our findings of increased atherosclerosis in female mice [23,24].

We next hypothesized that CD36 expression in the WAT may be contributing to the metabolic differences we observed as previous reports found that *Cd36$^{-/-}$* mice had lower body weights despite increased triglyceride levels [25]. While there was no difference in CD36 expression between male *CD11c-Cre$^+$ Fcgr2b$^{fl/fl}$* recipients and littermate controls, there was a near 50% reduction in CD36 on female ATMs (Fig. 4D). As a general marker of activation, we also examined MHC Class II expression on ATDCs and found that it was increased on *CD11c-Cre$^+$ Fcgr2b$^{fl/fl}$* recipients in both males and females (Fig. 4E). Collectively these data demonstrate that there is an increase in pro-inflammatory ATDCs in *CD11c-Cre$^+$ Fcgr2b$^{fl/fl}$* recipients with increased maturation and activation as measured by expression of MHC Class II.

3.5. A CD11c-conditional FcγRIIb KO alters hepatic liver storage and synthesis in a sex-dependent manner

Given the liver's role in cholesterol and TG storage and synthesis, we hypothesized that hepatic DCs may be involved in modulating serum lipid levels. The lipid fraction from liver segments was purified and

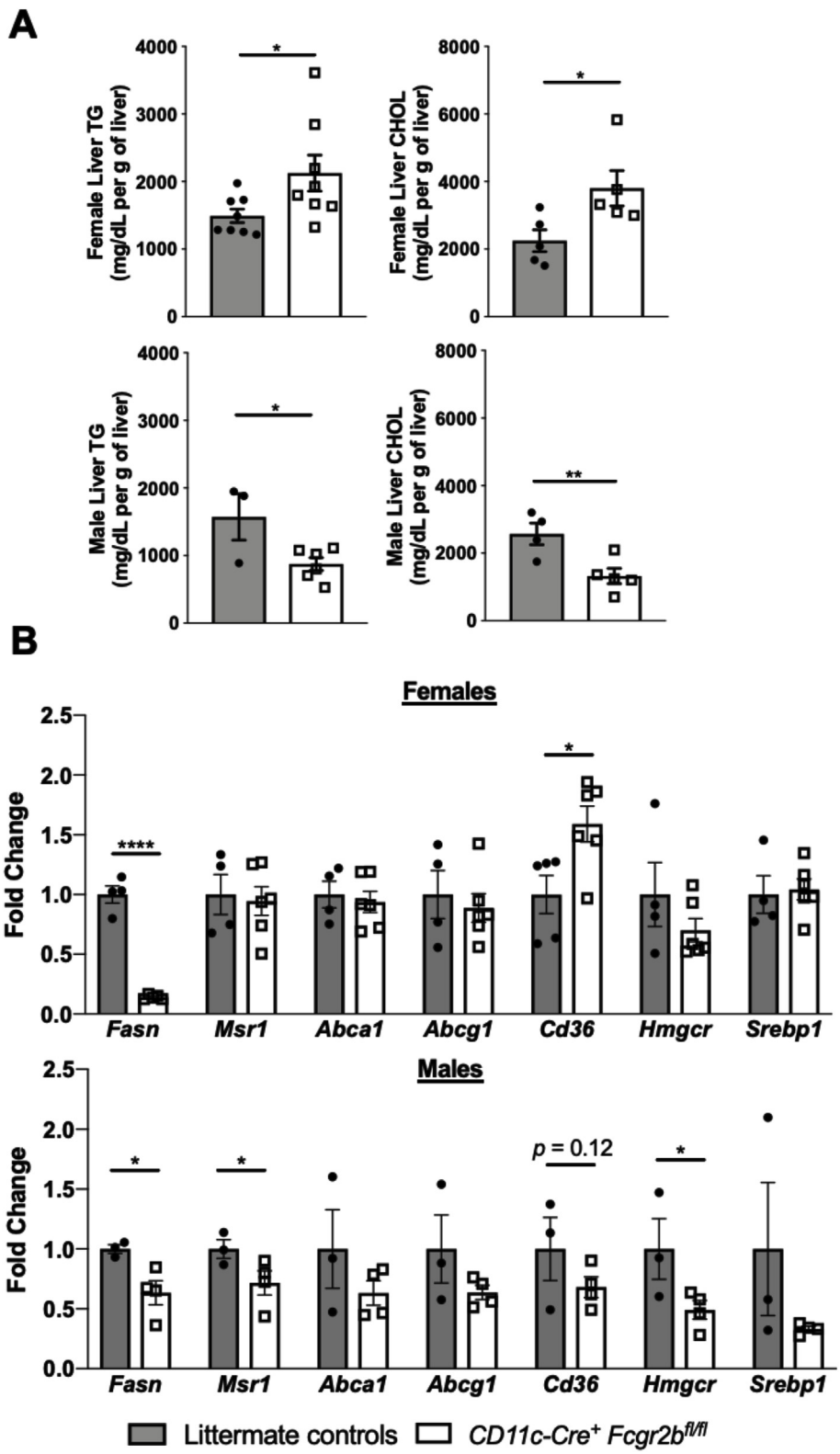

Fig. 5. Male and female *CD11c-Cre*$^{+}$ *Fcgr2b*$^{fl/fl}$ recipients produce less *Fasn* transcripts, but only female recipients store more cholesterol and triglycerides in their liver.
(A) Lipids were purified from male and female liver segments by the Folch method methods in 2:1 chloroform-methanol and triglycerides (TG) and cholesterol (CHOL) quantified by commercially available kits. (B) Quantitative real-time PCR was performed on liver segments to measure the expression of several genes involved in lipid synthesis and handling. Quantification was performed using the $2^{-\Delta\Delta CT}$ method and normalized to littermate controls. Error bars represent standard error. *, **, and **** indicates significance at $p < 0.05$, $p < 0.01$, and $p < 0.0001$ by Student's *t*-test.

cholesterol and TG content was quantified (Fig. 5A). In males, liver cholesterol and TG was lower in the *CD11c-Cre*$^{+}$ *Fcgr2b*$^{fl/fl}$ recipients compared to littermate controls. In contrast, female liver cholesterol and TG was increased in *CD11c-Cre*$^{+}$ *Fcgr2b*$^{fl/fl}$ mice. Therefore, liver lipid content was reflective of each sex's underlying atherosclerosis burden, but not their serum lipid profile.

We also processed whole liver segments for RNA to examine potential differences in hepatic lipid production and handling. Transcripts of fatty acid synthase (*Fasn)*, the key enzyme in synthesis of palmitate, were markedly reduced in both female and male *CD11c-Cre*$^{+}$ *Fcgr2b*$^{fl/fl}$ recipient livers compared to controls (Fig. 5B). Male *CD11c-Cre*$^{+}$ *Fcgr2b*$^{fl/fl}$ recipients also a reduction in other genes such HMG-CoA reductase (*Hmcgr*) in the cholesterol synthesis pathway and macrophage scavenger receptor-1 (*Msr1*) (Fig. 5B). Of note, there was

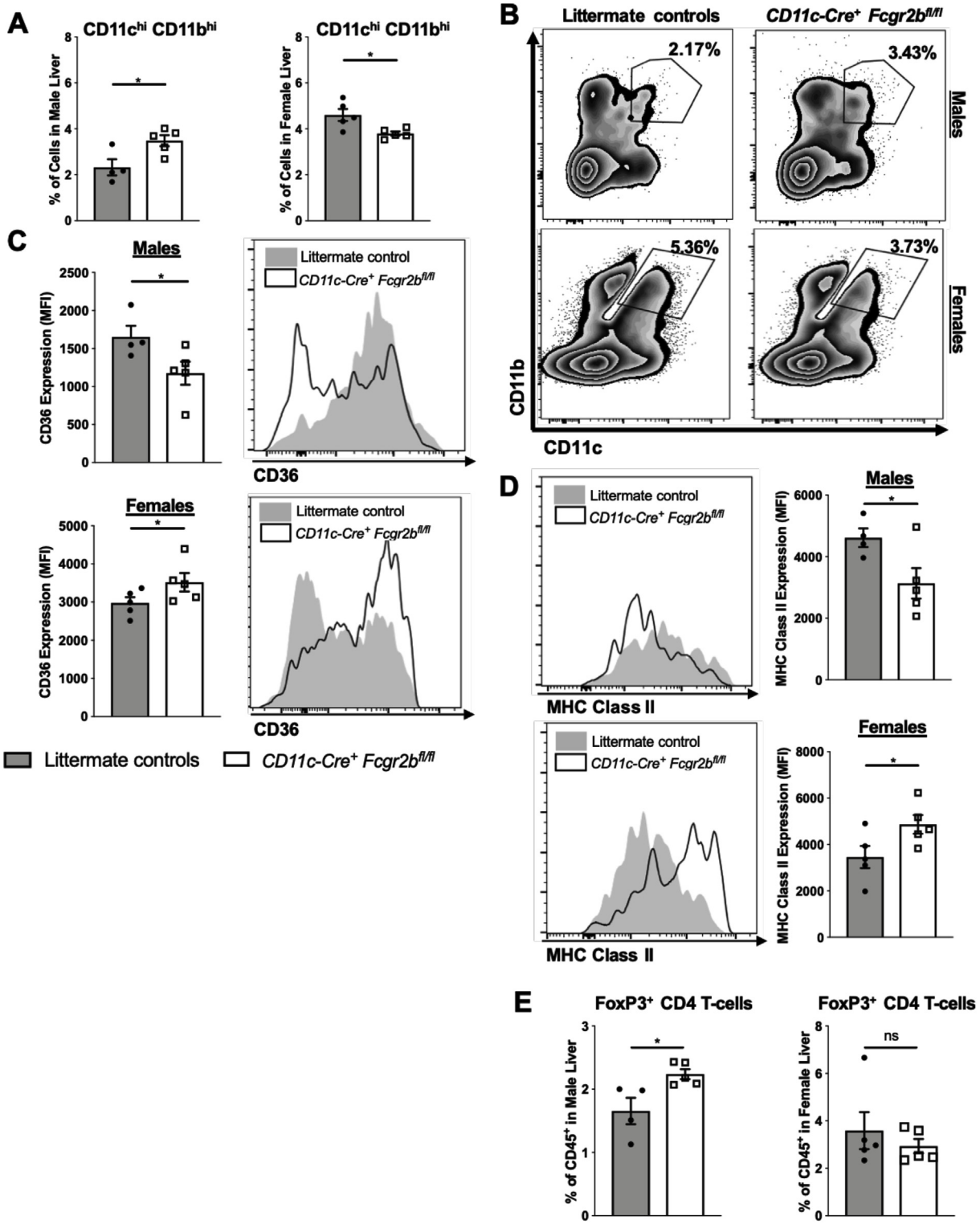

Fig. 6. Female, but not male, *CD11c-Cre^{+} Fcgr2b$^{fl/fl}$* recipients have increased MHC Class II and CD36 expression on liver DCs.
(A) Percent of CD11c^{hi} CD11b^{hi} cells in male (left) and female (right) livers was quantified by flow cytometric staining. (B) Representative contour plots of CD11c^{hi} CD11b^{hi} cells, gated on FSC and SSC. (C) Liver CD36 expression on CD11c^{hi} CD11b^{hi} cells quantitated by MFI for males and females. (D) Liver MHC Class II expression on CD11c^{hi} CD11b^{hi} cells quantitated by MFI for males and females. (E) Percent of T_{REGS} in male and female livers, quantified by gating on TCRβ^{+} CD4^{+} cells and intracellular FoxP3 staining. Data are representative of N = 4–5 mice per group. Error bars represent standard error. * indicates significance at $p < 0.05$ by Student's *t*-test.

significantly elevated hepatic *Cd36* transcripts in female *CD11c-Cre*$^{+}$ *Fcgr2b*$^{fl/fl}$ recipients with a slight trend towards reduced *Cd36* transcript levels in the males.

3.6. Female, but not male, CD11c-Cre^{+} Fcgr2b$^{fl/fl}$ recipients have increased MHC Class II and CD36 expression on liver DCs

We next sought to determine if there were differences in immune cells and markers of inflammation within the liver by flow cytometry. We found no differences in the total number of B-cells or CD4^{+} T-cells (data not shown) but did observe an increase in the percent of CD11c^{hi} CD11b^{hi} cells in male *CD11c-Cre*$^{+}$ *Fcgr2b*$^{fl/fl}$ recipients (Fig. 6A–B, Supplemental Fig. 6). Female recipients exhibited the opposite effect with a decrease in percent of CD11c^{hi} CD11b^{hi} cells. Given that cells from the liver have been previously shown to relocate to the aorta in *Ldlr*$^{-/-}$ mice [26], we were curious if the aorta would mimic the liver changes in CD11c^{hi} CD11b^{hi} cells. As predicted, we observed an increase in the percent of CD11c^{hi} CD11b^{hi} cells in the males and a trend towards decreased CD11c^{hi} CD11b^{hi} cells in the females. (Supplemental Figs. 7A–B).

Closer examination of the CD11c^{hi} CD11b^{hi} subset demonstrated that male mice had significantly less CD36 and MHC Class II expression with knockout of FcγRIIb, whereas females had an increase in the expression of both markers in the liver (Fig. 6C–D). CD86 levels trended towards increased expression on CD11c^{hi} CD11b^{hi} cells in *CD11c-Cre*$^{+}$ *Fcgr2b*$^{fl/fl}$ recipients but was not significant (data not shown).

Given that one of the major roles of DCs is to present antigen, we analyzed different T-cell populations in the liver. Since we did not see any differences in T_H1 and T_H17 populations (data not shown), we focused on liver-specific T_{REGS}, as previous studies have shown that hepatic T_{REG} populations are altered in hypercholesterolemia [26]. Furthermore, depletion of FoxP3^{+} populations increases serum cholesterol and TGs [26,27]. Livers from male *CD11c-Cre*$^{+}$ *Fcgr2b*$^{fl/fl}$ recipients had a larger percent of FoxP3^{+} T-cells than littermate controls (Fig. 6E). In contrast, female *CD11c-Cre*$^{+}$ *Fcgr2b*$^{fl/fl}$ recipients demonstrated no difference in the percent of FoxP3^{+} T-cells.

4. Discussion

The current study demonstrates sex-specific effects of a CD11c^{+} conditional FcγRIIb KO on atherogenesis. The observation that male *CD11c-Cre*$^{+}$ *Fcgr2b*$^{fl/fl}$ recipients had less atherosclerosis was surprising given the body of literature supporting an immunosuppressive role for FcγRIIb both *in vitro* and *in vivo*. [12,14,28,29] However, these studies do not specify the sex of the mice used during experimentation. Additionally, not all studies have observed a tolerance-inducing role for FcγRIIb [15,30]. Our results suggest that there are major sex differences in the effect of a CD11c-conditional FcγRIIb KO on atherosclerosis, and that this may be more tolerance-inducing in males and inflammation-promoting in females.

Estrogen is thought be protective against atherosclerosis, as females do not usually develop clinical CVD until after menopause. Hepatic lipid metabolism has been implicated as at least a partial causal agent as ovariectomized monkeys demonstrate increased hepatic cholesterol synthesis, hepatic cholesterol storage and consequently, increased atherosclerosis [31]. However, lipids are only one of the many mediators of atherosclerosis. The role of chronic inflammation in atherogenesis is now more highly recognized and there are marked sex-differences in the rates of autoimmune diseases. SLE, for example, affects ten times more females than males [32]. Estrogens are also a potential candidate for this bias as the onset of SLE is more frequent in women of childbearing age [32]. A recent study found that estrogens can increase DC maturation, enhance metabolic pathways in DCs, and modulate type I IFN-dependent and type I IFN-independent upregulation of DC activation markers in response to TLR stimulation [33]. Interestingly, estrogens have been shown to affect FcγR expression. Kramer et al. found that 17β-estradiol significantly regulated FcγRIII expression and subsequent cytokine release in monocytes via the estrogen receptor [34]. A separate study found that estrogen treatment of guinea pigs enhanced clearance of IgG-sensitized erythrocytes by increasing splenic-macrophage FcγR expression [35]. These studies combined with our data warrant further exploration into the ability of estrogen to regulate FcγRIIb.

Given the dramatic near 60% increase in atherosclerosis we observed in female *CD11c-Cre*$^{+}$ *Fcgr2b*$^{fl/fl}$ recipients despite significant lower serum cholesterol and triglyceride levels, we would hypothesize that the protective effect of estrogen on atherosclerosis and hepatic cholesterol metabolism is, in part, through FcγRIIb expression on CD11c^{+} cells. This is supported by our observation that when FcγRIIb is knocked down by even just 50% on CD11c^{+} cells, female mice had increased hepatic cholesterol and TG and increased markers of inflammation (i.e. SAA, MHC Class II expression). In males the role of FcγRIIb on CD11c^{+} cells in maintaining peripheral tolerance may be much less important in the absence of estrogen. Consequently, we would hypothesize that since our male mice did not experience an increase in liver cholesterol, TG or DC activation markers, the atheroprotective effect of the lower serum cholesterol and triglycerides predominated. We also observed increased serum anti-oxLDL IgM levels in male but not female CD11c-Cre^{+} recipients, which in several mouse and human studies was protective against atherosclerosis and is likely contributing to our phenotype [36].

Our data suggests that CD36 may be the mechanism by which FcγRIIb on CD11c^{+} cells modulates hepatic cholesterol and TG. Also known as fatty acid translocase, CD36, is a receptor for oxLDL and long chain fatty acids that is abundant in tissues active in fatty acid metabolism such as WAT, skeletal muscle, and cardiac muscle [25]. Interestingly, *Cd36*$^{-/-}$ mice are protected from atherosclerosis, insulin resistance, and obesity [37–39]. In several other diet-induced obesity studies or human studies of non-alcoholic fatty liver disease, hepatic CD36 levels have been found to be significantly elevated and this elevation correlated with increased liver TG storage [40,41]. Consistent with this, we found increased *Cd36* transcripts in whole liver lysates and increased CD36 expression on CD11c^{+} CD11b^{+} cells in female *CD11c-Cre*$^{+}$ *Fcgr2b*$^{fl/fl}$ recipients, which was the group with increased liver TGs and increased atherosclerosis. In addition to its role in metabolism, CD36 is also implicated in promoting inflammation. With cooperation from a TLR4/TLR6 heterodimer, CD36 was found to coordinate NLRP3 inflammasome activation and subsequent IL-1β production [42]. In DCs specifically, blocking CD36 with a monoclonal antibody inhibited LPS-induced DC maturation [43]. Instead of upregulation typical activation markers such as CD86 or secreting IL-12, IL-10 production from these DCs increased significantly. This was particularly interesting, given that we found more T_{REGS} present in the livers of male *CD11c-Cre*$^{+}$ *Fcgr2b*$^{fl/fl}$ recipients. Intrahepatic T_{REGS} are particularly important as they are capable of directly migrating to the aorta in *Ldlr*$^{-/-}$ mice [26]. T_{REGS} are critical in preventing atherosclerosis development, elegantly shown by Klingenberg et al. when they depleted FoxP3^{+} T_{REGS} by the diphtheria toxin and observed a 2.1 fold increase in atherosclerosis and a 1.7 fold increase in cholesterol and TGs [27]. They reported that liver lipoprotein catabolism was significantly altered by T_{REG} absence. Therefore, we would hypothesize that the decreased CD36 expression in the livers of male *CD11c-Cre*$^{+}$ *Fcgr2b*$^{fl/fl}$ recipients led to decreased activation markers on hepatic DCs, increased IL-10 production from the same DCs, and a subsequent atheroprotective increase in hepatic T_{REGS}.

The increase in CD11c^{+} CD11b^{+} cells in male *CD11c-Cre*$^{+}$ *Fcgr2b*$^{fl/fl}$ recipient livers was unexpected given literature reporting increases in liver DCs in obesity in inflammation [26,44]. However, Ibrahim et al. discovered two populations of liver DCs – those with high lipid content which were immunogenic and activated T-cells, and those with low lipid content which were tolerogenic and induced T_{REGS} [45]. Inhibiting DC fatty acid synthesis reduced DC immunogenicity [45]. This is

consistent with other reports that high cholesterol loading of CD11c$^+$ cells can trigger the development of autoimmunity [46]. Additionally, as MHC II peptide complexes cluster in cholesterol-dependent microdomains on the DC surface, cholesterol depletion often disrupts these clusters as well as the antigen-presentation function of the DCs [47]. We did not investigate the lipid content of liver DCs in this study but it would be an interesting avenue to pursue in the future as another group reported that liver DCs can contribute heavily to tolerance by active T-cell deletion [48].

To separate DCs and macrophages in WAT we used CD64, a commonly accepted marker to differentiate ATMs and ATDCs [23]. CD11c$^+$ ATMs are M1 like, more inflammatory, and are also more abundant in obese WAT [49]. A reduction in this population indicates a decrease in WAT inflammation and suggests an improvement in insulin resistance, which often correlates with atherosclerosis risk [49]. This is consistent with our observed decrease in male ATMs and decreased atherosclerosis. Similarly, females experienced no decrease in ATMs and were more prone to developing atherosclerosis. In contrast to WAT, we realize that there is still considerable overlap in macrophage and DC populations in the liver, blood, and aorta. Accordioning, the differences that we observed in these tissues could be due to macrophages expressing CD11c. This, however, not detract find the findings that highlight the importance of FcγRIIb on CD11c$^+$ cells during atherogenesis.

Despite sex-dependent differences in atherosclerosis, we unexpectedly found that both male and female *CD11c-Cre*$^+$ *Fcgr2b*$^{fl/fl}$ recipients had lower serum cholesterol and triglycerides. Previous evidence supports a role for CD11c$^+$ cells in cholesterol homeostasis. In one study, the DC population was expanded by overexpressing the antiapoptotic gene *hBcl-2* under the control of the CD11c promoter [50]. Despite finding enhanced T-cell activation in these mice, they found no increase in atherosclerosis due to a surprising atheroprotective decrease in serum cholesterol levels. The authors also reversed this effect by conjugating CD11c with the diphtheria toxin receptor to deplete DCs, thereby inducing hypercholesterolemia. However, no explanation has been reported for these effects. Our findings newly implicate FcγRIIb in this cholesterol lowering effect of CD11c$^+$ cells, likely through decreased expression of alteration of liver lipid synthesis genes such as *Fasn and Hmgcr*.

Another potential contributor to this phenomenon is that the cholesterol and TG is stored also being stored in fat. Interestingly, ATDCs have been implicated in influencing differentiation and development of adipocytes and we observed more ATDCs in both our male and female *CD11c-Cre*$^+$ *Fcgr2b*$^{fl/fl}$ recipients. However, GM-CSF deficient (*Csf2*$^{-/-}$) mice which had 75% fewer ATDCs had a 30% increase in whole body adiposity [51]. This would indicate that ATDCs actually restrict AT expansion. This is interesting given our observations that *CD11c-Cre*$^+$ *Fcgr2b*$^{fl/fl}$ recipients gained less weight overall, which could be in part due to the increase in ATDCs.

In conclusion, we saw two major effects of a CD11c-conditional FcγRIIb KO: a sex-dependent increase in inflammation causing enhanced atherosclerosis and a sex-independent decrease in serum cholesterol and TGs. Our results suggest that increased CD36 expression on hepatic DCs in the female *CD11c-Cre*$^+$ *Fcgr2b*$^{fl/fl}$ recipient livers may account for the increase in hepatic TG storage and subsequent increase in atherosclerosis. We found decreased expression of liver lipid synthesis genes, which highlights a novel role for FcγRIIb on CD11c$^+$ cells in regulating serum cholesterol and TG levels. Collectively these findings provide better insight into mechanism of FcγRIIb involvement in hypercholesteremia, obesity, insulin resistance, and atherosclerosis.

Conflicts of interest

The authors declared they do not have anything to disclose regarding conflict of interest with respect to this manuscript.

Author contributions

Jennifer Marvin performed the research, data analysis, and wrote the manuscript. Jillian P. Rhoads was involved in data collection. Amy S. Major contributed to study design and reviewed and edited the intellectual content.

Financial support

This work was supported by a grant from the Veterans Administration (Grant 101BX002968). J.M. was supported by Vanderbilt Medical Scholar Program.

Acknowledgements

We would like to thank Joseph A. Balsamo for his assistance feeding the mice, Brenna D. Appleton for her help during sac days, Wanying Zhu for her help running the FPLC, Jeffrey C. Rathmell for use of his MACSQuant, and Christopher T. Peek for reviewing and editing the manuscript.

Appendix A. Supplementary data

Supplementary data to this article can be found online at https://doi.org/10.1016/j.atherosclerosis.2019.04.221.

References

[1] E.J. Benjamin, S.S. Virani, C.W. Callaway, et al., Heart disease and stroke statistics-2018 update: a report from the American heart association, Circulation 137 (2018) e67–e492.
[2] M.F. Lopes-Virella, G. Virella, T.J. Orchard, et al., Antibodies to oxidized LDL and LDL-containing immune complexes as risk factors for coronary artery disease in diabetes mellitus, Clin. Immunol. 90 (1999) 165–172.
[3] L.W. Stanton, R.T. White, C.M. Bryant, et al., A macrophage Fc receptor for IgG is also a receptor for oxidized low density lipoprotein, J. Biol. Chem. 267 (1992) 22446–22451.
[4] J.P. Rhoads, J.R. Lukens, A.J. Wilhelm, et al., Oxidized low-density lipoprotein immune complex priming of the Nlrp3 inflammasome involves TLR and FcgammaR cooperation and is dependent on CARD9, J. Immunol. 198 (2017) 2105–2114.
[5] Y. Huang, A. Jaffa, S. Koskinen, et al., Oxidized LDL-containing immune complexes induce Fc gamma receptor I-mediated mitogen-activated protein kinase activation in THP-1 macrophages, Arterioscler. Thromb. Vasc. Biol. 19 (1999) 1600–1607.
[6] F. Nimmerjahn, J.V. Ravetch, Fcgamma receptors as regulators of immune responses, Nat. Rev. Immunol. 8 (2008) 34–47.
[7] P. Hernandez-Vargas, G. Ortiz-Munoz, O. Lopez-Franco, et al., Fcgamma receptor deficiency confers protection against atherosclerosis in apolipoprotein E knockout mice, Circ. Res. 99 (2006) 1188–1196.
[8] S. Bolland, J.V. Ravetch, Spontaneous autoimmune disease in FcγRIIB-deficient mice results from strain-specific epistasis, Immunity 13 (2000) 277–285.
[9] L.C. Willcocks, E.J. Carr, H.A. Niederer, et al., A defunctioning polymorphism in FCGR2B is associated with protection against malaria but susceptibility to systemic lupus erythematosus, Proc. Natl. Acad. Sci. U. S. A 107 (2010) 7881–7885.
[10] M. Mackay, A. Stanevsky, T. Wang, et al., Selective dysregulation of the FcgammaIIB receptor on memory B cells in SLE, J. Exp. Med. 203 (2006) 2157–2164.
[11] T.R. Radstake, B. Franke, M.H. Wenink, et al., The functional variant of the inhibitory Fcgamma receptor IIb (CD32B) is associated with the rate of radiologic joint damage and dendritic cell function in rheumatoid arthritis, Arthritis Rheum. 54 (2006) 3828–3837.
[12] Li, F, Smith, P and Ravetch, JV, Inhibitory Fcγ receptor is required for the maintenance of tolerance through distinct mechanisms, J. Immunol. (Baltimore, Md. : 1950), 2014;192:3021-3028.
[13] M.R. Clatworthy, C.E. Aronin, R.J. Mathews, et al., Immune complexes stimulate CCR7-dependent dendritic cell migration to lymph nodes, Nat. Med. 20 (2014) 1458–1463.
[14] N. van Montfoort, P.A. t Hoen, S.M. Mangsbo, et al., Fcgamma receptor IIb strongly regulates Fcgamma receptor-facilitated T cell activation by dendritic cells, J. Immunol. 189 (2012) 92–101.
[15] Y.V. Mendez-Fernandez, B.G. Stevenson, C.J. Diehl, et al., The inhibitory FcgammaRIIb modulates the inflammatory response and influences atherosclerosis in male apoE(-/-) mice, Atherosclerosis 214 (2011) 73–80.
[16] E.Y. Harmon, V. Fronhofer 3rd, R.S. Keller, et al., Anti-inflammatory immune skewing is atheroprotective: Apoe-/-FcgammaRIIb-/- mice develop fibrous carotid plaques, J Am Heart Assoc 3 (2014) e001232.
[17] H.P. Ng, X. Zhu, E.Y. Harmon, et al., Reduced atherosclerosis in apoE-inhibitory FcgammaRIIb-deficient mice is associated with increased anti-inflammatory

responses by T cells and macrophages, Arterioscler. Thromb. Vasc. Biol. 35 (2015) 1101–1112.
[18] B. Paigen, A. Morrow, P.A. Holmes, et al., Quantitative assessment of atherosclerotic lesions in mice, Atherosclerosis 68 (1987) 231–240.
[19] J. Folch, M. Lees, G.H.S. Stanley, A simple method for the isolation and purification of total lipids from animal tissues, J. Biol. Chem. 226 (1957) 497–509.
[20] J.S. Orr, A.J. Kennedy, A.H. Hasty, Isolation of adipose tissue immune cells, JoVE : JoVE (2013) 50707.
[21] R. Parker, The role of adipose tissue in fatty liver diseases, Liver Res. 2 (2018) 35–42.
[22] J.X. Sierra Rojas, M. García-San Frutos, D. Horrillo, et al., Differential development of inflammation and insulin resistance in different adipose tissue depots along aging in wistar rats: effects of caloric restriction, J. Gerontol. Series A: Biol. Sci. Med. Sci. 71 (2016) 310–322.
[23] K.W. Cho, B.F. Zamarron, L.A. Muir, et al., Adipose tissue dendritic cells are independent contributors to obesity-induced inflammation and insulin resistance, J. Immunol. 197 (2016) 3650.
[24] A. Bertola, T. Ciucci, D. Rousseau, et al., Identification of adipose tissue dendritic cells correlated with obesity-associated insulin-resistance and inducing Th17 responses in mice and patients, Diabetes 61 (2012) 2238.
[25] J.R. Goudriaan, V.E.H. Dahlmans, B. Teusink, et al., CD36 deficiency increases insulin sensitivity in muscle, but induces insulin resistance in the liver in mice, JLR (J. Lipid Res.) 44 (2003) 2270–2277.
[26] R.K.W. Mailer, A. Gistera, K.A. Polyzos, et al., Hypercholesterolemia induces differentiation of regulatory T cells in the liver, Circ. Res. 120 (2017) 1740–1753.
[27] R. Klingenberg, N. Gerdes, R.M. Badeau, et al., Depletion of FOXP3(+) regulatory T cells promotes hypercholesterolemia and atherosclerosis, J. Clin. Investig. 123 (2013) 1323–1334.
[28] R.M. Anthony, T. Kobayashi, F. Wermeling, et al., Intravenous gammaglobulin suppresses inflammation through a novel T(H)2 pathway, Nature 475 (2011) 110–113.
[29] D.D. Desai, S.O. Harbers, M. Flores, et al., Fc receptor IIB on dendritic cells enforces peripheral tolerance by inhibiting effector T cell responses, J. Immunol. 178 (2007) 6217–6226.
[30] A. Bergtold, D.D. Desai, A. Gavhane, et al., Cell surface recycling of internalized antigen permits dendritic cell priming of B cells, Immunity 23 (2005) 503–514.
[31] K. Kavanagh, M.A. Davis, L. Zhang, et al., Estrogen decreases atherosclerosis in Part By reducing hepatic acyl-CoA:cholesterol acyltransferase 2 (ACAT2) in monkeys, Arterioscler. Thromb. Vasc. Biol. 29 (2009) 1471–1477.
[32] L. Lisnevskaia, G. Murphy, D. Isenberg, Systemic lupus erythematosus, Lancet 384 (2014) 1878–1888.
[33] M.H. Lee, M. Chakhtoura, U. Sriram, et al., Conventional DCs from male and female lupus-prone B6.NZM sle1/sle2/sle3 mice express an IFN signature and have a higher immunometabolism that are enhanced by estrogen, J. Immunol. Res. 2018 (2018) 1601079.
[34] P.R. Kramer, V. Winger, S.F. Kramer, 17beta-Estradiol utilizes the estrogen receptor to regulate CD16 expression in monocytes, Mol. Cell. Endocrinol. 279 (2007) 16–25.
[35] F. Gomez, P. Ruiz, J.A. Bernal, et al., Enhancement of splenic-macrophage Fcgamma receptor expression by treatment with estrogens, Clin. Diagn. Lab. Immunol. 8 (2001) 806–810.
[36] J. Zhang, D. Wang, S. He, Roles of antibody against oxygenized low density lipoprotein in atherosclerosis: recent advances, Int. J. Clin. Exp. Med. 8 (2015) 11922–11929.
[37] T. Hajri, X.X. Han, A. Bonen, et al., Defective fatty acid uptake modulates insulin responsiveness and metabolic responses to diet in CD36-null mice, J. Clin. Investig. 109 (2002) 1381–1389.
[38] D.J. Kennedy, S. Kuchibhotla, K.M. Westfall, et al., A CD36-dependent pathway enhances macrophage and adipose tissue inflammation and impairs insulin signalling, Cardiovasc. Res. 89 (2011) 604–613.
[39] M. Febbraio, E.A. Podrez, J.D. Smith, et al., Targeted disruption of the class B scavenger receptor CD36 protects against atherosclerotic lesion development in mice, J. Clin. Investig. 105 (2000) 1049–1056.
[40] D.P. Koonen, R.L. Jacobs, M. Febbraio, et al., Increased hepatic CD36 expression contributes to dyslipidemia associated with diet-induced obesity, Diabetes 56 (2007) 2863–2871.
[41] M.E. Miquilena-Colina, E. Lima-Cabello, S. Sanchez-Campos, et al., Hepatic fatty acid translocase CD36 upregulation is associated with insulin resistance, hyperinsulinaemia and increased steatosis in non-alcoholic steatohepatitis and chronic hepatitis C, Gut 60 (2011) 1394–1402.
[42] F.J. Sheedy, A. Grebe, K.J. Rayner, et al., CD36 coordinates NLRP3 inflammasome activation by facilitating intracellular nucleation of soluble ligands into particulate ligands in sterile inflammation, Nat. Immunol. 14 (2013) 812–820.
[43] B.C. Urban, N. Willcox, D.J. Roberts, A role for CD36 in the regulation of dendritic cell function, Proc. Natl. Acad. Sci. U. S. A. 98 (2001) 8750–8755.
[44] M. Stefanovic-Racic, X. Yang, M.S. Turner, et al., Dendritic cells promote macrophage infiltration and comprise a substantial proportion of obesity-associated increases in CD11c cells in adipose tissue and liver, Diabetes 61 (2012) 2330.
[45] J. Ibrahim, A.H. Nguyen, A. Rehman, et al., Dendritic cell populations with different concentrations of lipid regulate tolerance and immunity in mouse and human liver, Gastroenterology 143 (2012) 1061–1072.
[46] A. Ito, C. Hong, K. Oka, et al., Cholesterol accumulation in CD11c(+) immune cells is a causal and targetable factor in autoimmune disease, Immunity 45 (2016) 1311–1326.
[47] B. Bosch, E.L. Heipertz, J.R. Drake, et al., Major histocompatibility complex (MHC) class II-peptide complexes arrive at the plasma membrane in cholesterol-rich microclusters, J. Biol. Chem. 288 (2013) 13236–13242.
[48] A. Goubier, B. Dubois, H. Gheit, et al., Plasmacytoid dendritic cells mediate oral tolerance, Immunity 29 (2008) 464–475.
[49] D. Patsouris, P.P. Li, D. Thapar, et al., Ablation of CD11c-positive cells normalizes insulin sensitivity in obese insulin resistant animals, Cell Metabol. 8 (2008) 301–309.
[50] E.L. Gautier, T. Huby, F. Saint-Charles, et al., Conventional dendritic cells at the crossroads between immunity and cholesterol homeostasis in atherosclerosis, Circulation 119 (2009) 2367–2375.
[51] N. Pamir, N.C. Liu, A. Irwin, et al., Granulocyte/macrophage colony-stimulating factor-dependent dendritic cells restrain lean adipose tissue expansion, J. Biol. Chem. 290 (2015) 14656–14667.